Keratins significantly contribute to cell stiffness and impact invasive behavior

Kristin Seltmann[a,1], Anatol W. Fritsch[b,1], Josef A. Käs[b,2], and Thomas M. Magin[a,2]

[a]Translational Center for Regenerative Medicine and Institute of Biology, and [b]Fakultät für Physik und Geowissenschaften, Abteilung Physik der Weichen Materie, Universität Leipzig, 04103 Leipzig, Germany

Edited by David A. Weitz, Harvard University, Cambridge, MA, and approved August 9, 2013 (received for review June 5, 2013)

Cell motility and cell shape adaptations are crucial during wound healing, inflammation, and malignant progression. These processes require the remodeling of the keratin cytoskeleton to facilitate cell–cell and cell–matrix adhesion. However, the role of keratins for biomechanical properties and invasion of epithelial cells is only partially understood. In this study, we address this issue in murine keratinocytes lacking all keratins on genome engineering. In contrast to predictions, keratin-free cells show about 60% higher cell deformability even for small deformations. This response is compared with the less pronounced softening effects for actin depolymerization induced via latrunculin A. To relate these findings with functional consequences, we use invasion and 3D growth assays. These experiments reveal higher invasiveness of keratin-free cells. Reexpression of a small amount of the keratin pair K5/K14 in keratin-free cells reverses the above phenotype for the invasion but does not with respect to cell deformability. Our data show a unique role of keratins as major players of cell stiffness, influencing invasion with implications for epidermal homeostasis and pathogenesis. This study supports the view that down-regulation of keratins observed during epithelial–mesenchymal transition directly contributes to the migratory and invasive behavior of tumor cells.

cell mechanics | intermediate filaments | optical stretcher | Boyden chamber

Cell shape and tissue integrity largely depend on the cytoskeleton, which in mammals is composed of actin filaments, microtubules (MTs), and intermediate filaments (IFs). Together, they provide resilience against force, coordinate cell motility, mediate intracellular movements, and are involved in cell signaling (1, 2). Although mechanical resilience is of importance for the integrity of whole tissues, it is reasonable that for processes such as migration of cells out of dense tissues, single cells need to be highly deformable. The role of actin filaments and MTs is relatively well understood. However, the understanding of the respective contribution of IFs, encoded by a gene family of >70 members in humans and mice, to cell deformability, migration, and signaling is only beginning to emerge (2).

The IF cytoskeleton of epithelia is composed of keratins that assemble from heterodimers of at least one type I and type II keratin into long, apolar IFs. It is believed that the cell type– and differentiation state–specific expression of keratin isotypes contributes significantly to micromechanical properties of epithelial tissues (2). Basal epidermal keratinocytes express the keratin pair K5/K14, which are replaced by K1/K10 during skin differentiation, whereas tissue regeneration is accompanied by transient K6/K16 up-regulation and repression of K1/K10 (3). The occurrence of cell fragility diseases caused by keratin mutations, followed by collapse of the keratin cytoskeleton, has suggested a major contribution of keratins to cell and tissue integrity, although the underlying pathomechanisms are not yet understood (4). Furthermore, loss of keratin expression, together with down-regulation of cell–cell and cell–matrix contacts, represents an important feature of the epithelial–mesenchymal transition (EMT) and is thought to contribute to the increased migratory and invasive behavior of metastatic tumor cells. Their properties, which include active cell shape changes and increasing cell softness in tumor cells, rely largely on cell deformability as cells have to transmigrate their surrounding tissue (5–7).

For small deformations imposed on cells, cortical actin is generally seen as the dominant contributor to cell stiffness (8–10). Surprisingly, MTs are reported to have little or no significant effect on cell stiffness in this regime (11, 12). Based on the viscoelastic properties of IFs in vitro, it was suggested that they might be important for cell integrity at large deformations (13). Supporting this hypothesis, studies on vimentin-deficient cells revealed that they were less stiff than WT cells at high stresses, whereas for low stresses, there seemed to be no significant influence (14). Until now, the contribution of keratins to cell stiffness has not been fully examined.

To investigate the overall contribution of the keratin IF cytoskeleton to cell stiffness and invasive behavior, we generated keratinocyte cell lines devoid of the entire keratin cytoskeleton, together with a rescue cell line reexpressing the single keratin pair K5/K14 (3, 15). Based on measurements in a microfluidic optical stretcher analyzing the noncontact deformability of statistically relevant numbers of keratin-deficient, WT, and rescue cells (16), we identify a major contribution of the keratin cytoskeleton to whole cell deformability, which we show is significantly greater than that of actin for small deformations. Moreover, we show using a Boyden chamber assay and 3D tissue culture that loss of keratins enhances invasive behavior of keratinocytes, which can

Significance

In many processes such as wound healing, inflammation, and cancer progression, the cytoskeleton is influencing cell motility and cell shape. Thus far, in contrast to the actin and microtubule cytoskeleton, intermediate filament proteins are not well investigated in this context. Here, we show that keratin-free cells from mice skin lacking all keratins on genome engineering have about 60% higher cell deformability even for small deformations in contrast to a smaller effect generated by actin depolymerization. Keratin-free cells are more invasive and show an increased growth in a 3D assay. Our study highlights keratins' role in cell stiffness and its influence in invasion, supporting the view that down-regulation of keratins observed during epithelial–mesenchymal transition directly contributes to the migratory and invasive behavior of tumor cells.

Author contributions: K.S., A.W.F., J.A.K., and T.M.M. designed research; K.S. and A.W.F. performed research; K.S. and A.W.F. contributed new reagents/analytic tools; K.S. and A.W.F. analyzed data; and K.S., A.W.F., J.A.K., and T.M.M. wrote the paper.

The authors declare no conflict of interest.

This article is a PNAS Direct Submission.

[1]K.S. and A.W.F. contributed equally to this work.

[2]To whom correspondence may be addressed. E-mail: jkaes@physik.uni-leipzig.de or thomas.magin@trm.uni-leipzig.de.

This article contains supporting information online at www.pnas.org/lookup/suppl/doi:10.1073/pnas.1310493110/-/DCSupplemental.

be significantly reduced by restoring only small amounts of keratin K5/K14.

Results

Strongly Increased Softening in Keratin-Free Cells. To investigate the contribution of keratins to epithelial cell mechanics, we established a keratinocyte cell line lacking all type II keratins. In accordance with the instability of type I keratins in the absence of type II keratin partners, this resulted in cell lines completely lacking keratin filaments, without compensatory up-regulation of other IF proteins (15, 17). To verify the keratin dependence of the resulting phenotypes, a rescue keratinocytes cell line reexpressing K5/K14 filaments stably was developed (named K5 cells), which expresses 13% of the keratin protein amount of the WT (15). Thus, it is possible to investigate the overall biomechanical contribution of the keratin cytoskeleton in living epithelial cells. To probe whole cell mechanical properties, we use an automated microfluidic optical stretcher (μOS), a two-beam laser trap that deforms single suspended cells with optically induced surface forces (Fig. 1*A*) (16). On a stepwise increase of the laser power (stretch), the cells start to deform and display creep behavior $J(t)$ followed by relaxation after a subsequent stepwise decrease of the laser power. Addressing the variability of biological samples, a minimum of 300 cells for each cell line was used for analysis. As a measure of the mechanical properties, we analyzed the median creep deformation J (t = 3 s) at the end of cell stretching. Comparison of WT and KO cells revealed a drastic increase of cell deformability of about 60 ± 20% for the KO cells (Fig. 1*C*). At the same time, deformation curves and J (t = 3 s) for KO and K5 rescue cells are similar and lie within each other's confidence bounds (Fig. 1 *B* and *C*). Due to the low expression level of keratin protein of 13% in K5 cells, the similar deformation curves are to be expected, suggesting that epithelial cell stiffness critically depends on the amount of keratin per cell.

The strong reliance on whole cell deformability on keratins could easily be caused by changes in the architecture and/or amount of other cytoskeletal components. To rule these out, we used immunofluorescence and Western blots to characterize the various cell lines for keratin, actin, and tubulin. Absence of keratin filaments can clearly be seen in KO keratinocytes, whereas

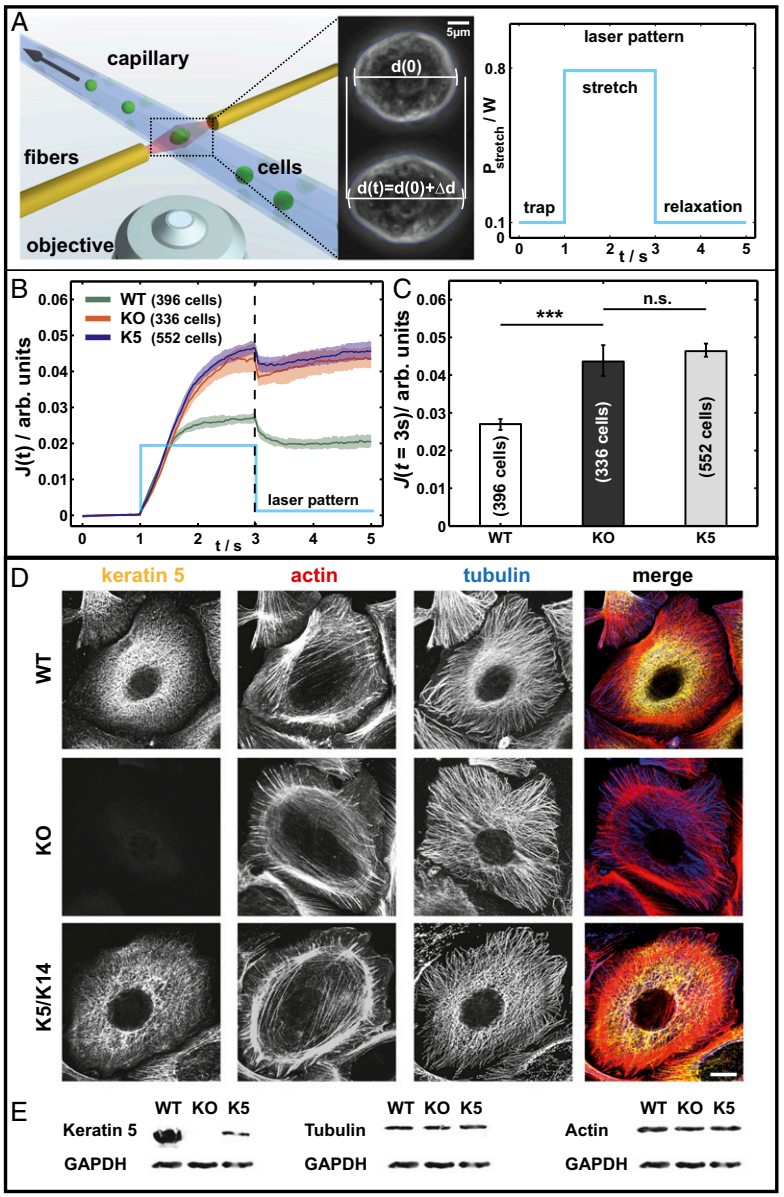

Fig. 1. Keratins are major determinants of cell stiffness. (*A*) (*Left*) Schematic of the μOS setup showing a strongly deforming KO cell treated with LatA. (*Right*) Laser pattern used for all μOS measurements. (*B* and *C*) Data sets from optical stretcher measurements of keratin-free and K5/K14 reexpressing cells compared with WT cells. Characterized by creep deformation curves $J(t)$ (*B*) and J (t = 3 s) (*C*) (***$P < 0.001$). (*D*) Immunofluorescence analysis using keratin and tubulin antibodies and phalloidin staining (actin). (*E*) Keratin 5, tubulin, and actin expression detected by Western blotting of total protein lysates. (Scale bar, 10 μm.)

K5 cells again form long keratin filaments. Additionally, immunofluorescence staining shows that actin and tubulin organization appears very similar in WT, KO, and K5 keratinocytes (Fig. 1*D*). Interestingly, F-actin distribution is not notably influenced by the keratin status under the culture conditions used here, and all cell lines displayed cortical cytoplasmic stress fibers in a similar arrangement. The actin and tubulin expression levels are equal in the cells as well (Fig. 1*E*). In addition, immunostaining for suspended cells was done to confirm a similar cytoskeletal structure of actin and microtubules in WT, KO, and K5 cells for conditions like in the μOS (Fig. S1).

Influence of F-Actin in Cell Stiffness. For small deformations, the cortical layer of the semiflexible polymer actin is often denoted as a major contributor to the mechanical properties of cells (8–10), whereas the reverse is proposed for keratin influence (9). Additionally, numerous studies proposed close interactions between actin and keratin cytoskeletons in many cells (18, 19). To dissect the relative contribution of actin and keratin cytoskeletons to cell deformability, WT and KO keratinocytes were treated with the F-actin depolymerizing drug latrunculin A (LatA; 0.25 μM) for 8 h before and during measurements. This treatment significantly altered the F-actin cytoskeleton, whereas overall organization of keratin filaments and the microtubule network remained largely unaffected (Fig. 2*C*). As expected, actin stress fibers were depolymerized, and most filamentous actin disappeared in all cell lines (Fig. 2*B*). Deformation of LatA-treated keratinocytes measured with the μOS revealed a significant increase of deformability in all cell types. For WT+LatA compared with WT cells, an increase of about 10 ± 10% was found, whereas both KO+LatA and K5+LatA cells showed an increase of about 20 ± 10% in comparison with their controls (Fig. 2*A*). Most importantly, the differences between WT+LatA and KO+LatA cells were still remarkable, with about 80 ± 20% higher relative deformation for the latter, independent of the depolymerization of the actin cytoskeleton. Regarding the curve shape of $J(t)$ of all LatA-treated cells, a qualitative change compared with controls was seen. This difference is most obvious on normalizing the deformation curves to the maximal deformation at J (t = 3 s) (Fig. 2*B*). All cell types treated with LatA showed the same curve shape, indicating the same underlying biomechanical behavior. Although this is true for LatA-treated cells, the creep curves of untreated controls display different curve shapes for WT compared with KO and K5 cells (Fig. 2*B*).

Deformability Increases Invasion and Enhances 3D Growth in a Colony Assay. In relation to the drastic impact of keratins seen for small deformations, we asked whether increased deformability of keratin-deficient keratinocytes affected their invasive behavior. During invasion, cells are exposed to a variety of mechanical cues such as shear stress and deformation, requiring adaptations of cell shape and adhesion mediated by the cytoskeleton (5). To test this, keratinocyte invasion was examined in a Boyden chamber assay in which cells have to squeeze through pores, forcing drastic deformation (6). Interestingly, the number of invading cells was 60 ± 7% higher among keratin-free cells compared with control cells (Fig. 3*A*; Movies S1, S2, and S3). To exclude proliferation effects in the invasion, proliferation was determined and showed no difference between all cell types (Fig. 3*B*). To visualize keratinocytes successfully invading the pores following the invasion

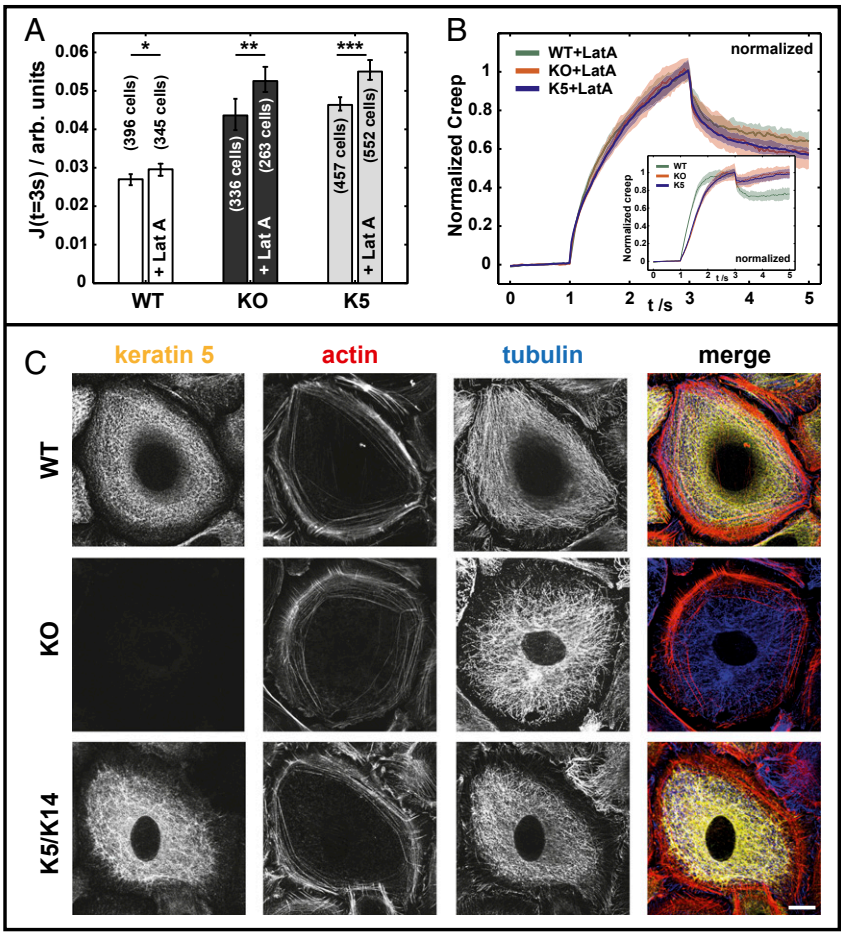

Fig. 2. LatA treatment enhances cell softness. (*A*) μOS data of WT, KO, and K5 cells in comparison with LatA-treated cells and respective cell counts (***$P < 0.001$; **$P < 0.01$; *$P < 0.05$). (*B*) Normalized creep curves of LatA treated and untreated cells (*Inset*). (*C*) LatA-treated cells immunostained for cytoskeletal proteins keratin 5, α-tubulin, and actin (phallodin). (Scale bar, 10 μm.)

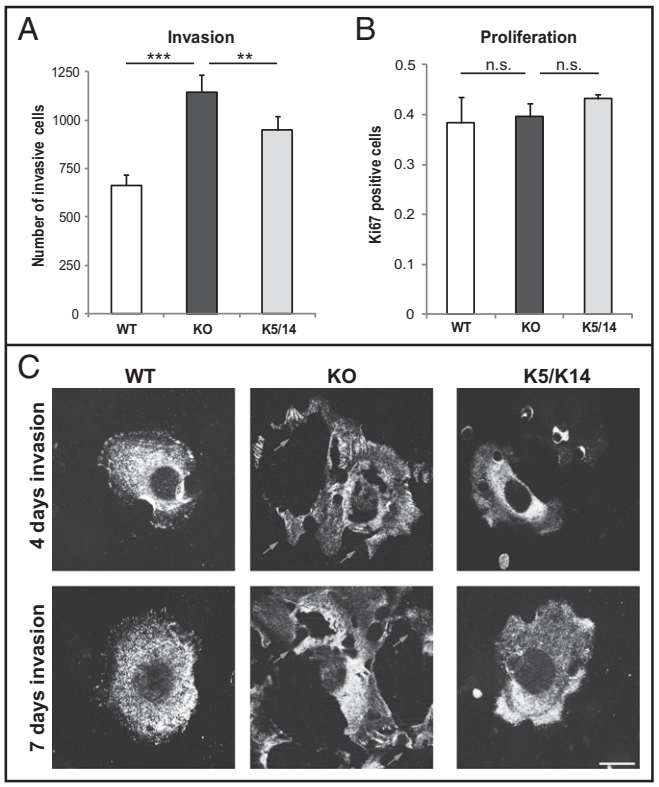

Fig. 3. Loss of keratins promotes invasion. (*A*) Quantification of transwell invasion experiments. The mean number of invaded cells per transwell membrane is presented. (*B*) Proliferation assay of keratinocytes following Ki67 staining. Error bars represent SD of three independent experiments. (*C*) Immunofluorescence analysis of cells having completed invasion at the bottom of the transwell membrane stained for vinculin at day 4 and day 7 (***$P < 0.001$ **$P < 0.01$). (Scale bar, 10 μm.)

process, the focal adhesion-associated protein vinculin was stained (Fig. 3*C*). After invasion, WT and K5 keratinocytes were smaller and less spread compared out of the pores with keratin-free cells, suggesting a faster invasion of KO cells even at day 7. Moreover, during the invasion process, living keratin-deficient KO cells frequently ruptured, leaving remnants behind them (Fig. 3*C*, arrows). In contrast, WT and K5 cells remained intact throughout the invasion process. Furthermore, the growth of keratinocytes in a 3D environment depending on the stress field imposed by the surrounding matrix was investigated. Single cells were embedded in an extracellular matrix and allowed to form colonies. In comparison with WT and K5 cells, keratin-free keratinocytes formed much larger colonies (Fig. 4*A*). Whereas colonies consisting of WT and K5 cells displayed regular shapes and well-organized cells, colonies from keratin-free keratinocytes grew on top of each other in a disorganized fashion (Fig. 4*B*). In addition, KO keratinocytes showed areas where cells move out of the colonies, whereas WT and K5 colonies stay compact (Fig. 4 *B* and *C*, arrows). Together with the findings from the Boyden chamber assay, this suggests that loss of the keratin cytoskeleton promotes acquisition of an invasive EMT-like state in murine keratinocytes.

Discussion

Although actin and microtubules are considered to be most important for biomechanical properties of cells, IF proteins were ignored for a long time in this field, owing to their insolubility in buffers of physiological strength and their redundancy (14, 20, 21). The elastic properties of IFs are illustrated by the fact that they can stretch three times their initial length before yielding, which are conditions where F-actin would already be irreversibly disrupted (22, 23). Previously, for the IF vimentin, it was shown by transfection of different desmin variants in fibroblasts that the rearrangements of IF can change the nanomechanical properties of these cells (24).

Our raw data represented through the deformation curves convincingly show that keratins significantly contribute to the mechanical properties of keratinocytes. A simple effective spring and dashpot model with three parallel independent springs representing the elastic contributions of keratin, actin, and other filaments was used and combined with a joint viscous background determined by the fluid cytoplasm (Fig. S2). This model allows us to estimate that the contribution of keratins to the elastic strength with respect to actin and other filaments can be described by the ratio 0.42:0.04:0.54, respectively, which shows that keratin is a significant player in the stability in cells (Table S1; Fig. S2). More accepted models, such as a glassy cell model that result in scaling laws represented here by a modified power law model described previously by Maloney et al. (25), also capture the significant contribution of keratins (Table S1).

Looking at the much lower bending stiffness of keratin compared with actin filaments, classical physical models would predict no major contribution of keratins in small deformation experiments. Using keratinocytes that express their normal set of keratins (WT), lack all keratins (KO), or contain one keratin pair K5/K14 (K5), we used a μOS to analyze the noncontact deformability of these cells. The data presented in this work show a drastic increase in creep deformation J ($t = 3$ s) of ~60% for the KO cells compared with WT cells, even for small deformations. Furthermore, WT and KO cells treated with the actin depolymerizing agent LatA show significant softening of ~10% and ~20%, respectively, which is much less compared with the effect of keratin IFs. In the absence of actin induced by LatA treatment,

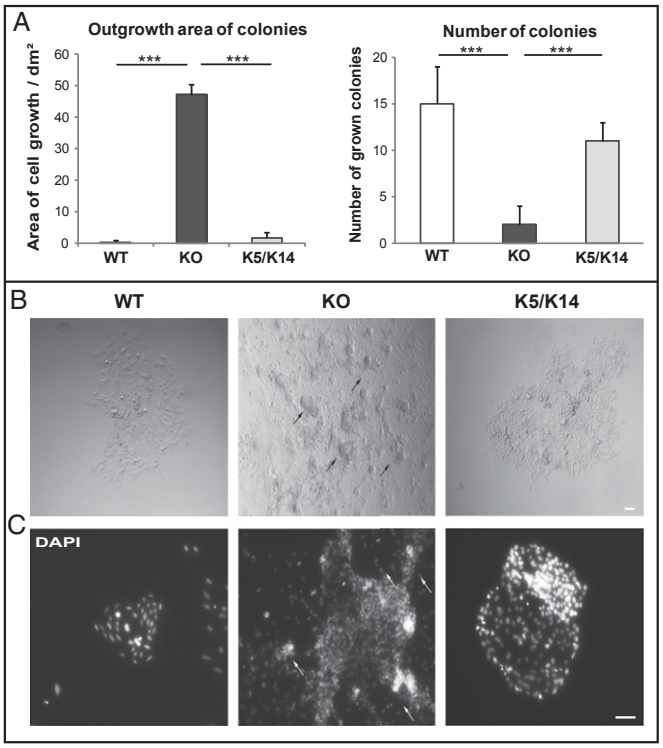

Fig. 4. Increased formation of colonies in keratin-free cells. (*A*) Formation of colonies surrounded by Matrigel. (*B*) Phase contrast images of cells growing in a 3D environment. (*C*) Colony assay stained using DAPI (***$P <$ 0.001). (Scale bar, 100 μm.)

cells show deformation curves with joint characteristics that are most likely dominated by the biomechanical features of the keratin cytoskeleton (Fig. 2*B*).

Regarding interconnection via linker protein connections between the actin and keratin filament networks, a group of proteins interacting with IFs called plakins and armadillo proteins are candidates for linkage (26–28), in particular, plectin isoforms (29–31). We can use our data to hypothesize about the strength of the coupling between actin and keratin. When disrupting the actin filaments with LatA, we see nearly the same relative effect between LatA-treated and -untreated WT and KO cells. Additionally, the relative effect of the keratin KO is similar comparing WT to KO with WT+LatA to KO+LatA. Taken these two findings, the coupling, e.g., via plectin cross-links, between actin and keratin filaments is quite weak for the cells presented in this study. Thus, the keratin and actin cytoskeleton mostly contribute independently to the cell elastic strength, which in part explains why the simple effective model of three independent springs for keratins, actin, and remaining filaments describes our data so well (Fig. S3; Table S1).

A previous study on immortalized patient cells containing a genetic keratin mutation (K14 R125P) compared with immortalized normal keratinocytes already raised the expectation that a total loss of keratins could have an influence on cell stiffness (12). In contrast, we directly compare the contribution of keratins in epithelial cell mechanics in keratinocytes expressing or lacking distinct sets of keratins. Additionally, because of the automated μOS, we have access to a statistical amount of single cell experiments that were shielded from the influence of additional parameters like adhesion to an artificial 2D matrix. For rescue cells (K5) with ∼13% the amount of keratin found in WT cells, we recorded the same deformation behavior as for KO cells; however, the invasive phenotype was nearly restored, resembling that of WT cells. Furthermore, our data also show that migration and adhesion properties were rescued in K5 cells (15).

In addition, we found an increased number of invading keratin-deficient cells and enhanced 3D growth in a colony assay, which was partially rescued by reexpression of K5. However, KO cells were ruptured during the invasion process, indicating mechanical instability of single cells in the absence of keratins. Our findings provide the basis for understanding pathomechanisms of the blistering skin disease epidermolysis bullosa simplex (EBS), caused by missense mutations in K5 or K14. In severe EBS, keratin missense mutations enforce collapse of an intact cytoskeleton into cytoplasmic aggregates, assumed to lead to a fragile epidermis (3, 32). In EBS, mechanical stress exposure leads to a ruptured epidermis with skin blisters, underlining the crucial role of keratin filaments in the mechanical stability of the skin (33–35). Our data strongly support the need to express a sufficiently high level of intact keratins to restore the biomechanical properties of keratinocytes and epidermis. Furthermore, loss of the keratin cytoskeleton reduced cell stiffness and therefore the enhanced cell deformability needed to squeeze through porous membranes used in an invasion assay. This approach is reminiscent of invasive cells at the tumor front (36). In this setting, altered expression is believed to contribute to the increased softness of tumorigenic cells and their state of malignancy (37, 38). On the other hand, increased softness might render tumor cells more susceptible to shear forces, selecting against cells that are too soft. In many cancers, cell shape changes are indicators of neoplastic transformation. Here, we show that the loss of keratin intermediate filament cytoskeleton, like in pathological processes, drastically affects invasion and 3D growth. In line, the keratin expression pattern is altered in tumorigenesis and can be used as prognostic marker, which can be related to biomechanical changes in this context (38). Also, in wounding, the keratin isotypes are switched to K6/K16 expression, suggesting keratins change migratory and biomechanical properties of such cells (39–41). Our results are in line with data showing that reorganization of keratin filaments leads to biomechanical changes and enhanced invasion (42). The notion that expression of 13% of total keratins in K5 cells did not significantly affect cell stiffness in μOS measurements but diminished invasion in a 3D assay most likely reflects exposure time to the mechanical force, which is very different between the two assays. Furthermore, the length of time allows induction of proinvasive signaling pathways in keratin-deficient keratinocytes (43).

In summary, we show using the optical stretcher, that the keratin cytoskeleton is a major contributor to cell stiffness and decreases cell invasiveness. Based on the findings reported here and elsewhere (7), we suggest that, by providing cell stiffness and maintaining desmosome-dependent intercellular adhesion, keratins assist in the maintenance of the epithelial phenotype and protect epithelial cells against acquisition of a metastatic phenotype.

Materials and Methods

Cell Culture and Drug Treatment. Isolation and culture of mouse keratinocytes of various genotypes were described previously (15, 17). Briefly, cells were grown in chelex-treated FAD medium (DMEM/Ham's F12, 3.5:1.1) supplemented with 10% (vol/vol) FCS Gold (PAA, chelex-treated), 0.18 mM adenine, 0.5 μg/mL hydrocortisone, 5 μg/mL insulin, 100 pM cholera toxin (all Sigma), 10 ng/mL EGF, 100 U/mL sodium pyruvate, 100 μg/mL penicillin/streptomycin, and 2 mM Glutamax (all Invitrogen), 5% CO_2 at 32 °C. Cells were cultured on collagen I (Invitrogen)-coated cell culture dishes. Cells were treated for 8 h with 0.25 μM LatA (Sigma Aldrich).

Antibodies. Antibodies used were mouse anti-vinculin (Sigma Aldrich), mouse anti–α-tubulin (Sigma Aldrich), and guinea pig anti-keratin 5 (44). Secondary antibodies conjugated to fluorochromes and PromoFluor-488–conjugated phalloidin were purchased from Dianova and Promokine.

Immunofluorescence Analysis. Staining conditions and image processing were described previously (7). Briefly, cells were fixed for 10 min in 4% formalin/PBS and incubated with primary antibodies for 1 h. All antibodies were diluted in TBS containing 1% BSA. Afterward, cells were incubated with the secondary antibody for 30 min and mounted with mounting medium (Dianova). Images were acquired using an AxioImager Z2 equipped with Zeiss Plan-Apochromat 63×/1.46 oil and Zeiss LSM 780 confocal microscope with 40×/1.3 NA or 63×/1.46 NA. Image analysis and processing were performed using the AxioVision 4.8 and Zen Software 2010 (Zeiss).

Invasion and Colony Assay. Invasion chambers for the transwell assay were prepared by coating 12-well inserts (Millipore) with growth factor–reduced Matrigel (BD Biosciences). Invasion assay plates were incubated for 4–7 d. Following incubation, the noninvading cells were removed by scrubbing the upper surface of the insert. The cells on the lower surface of the insert were fixed and stained with DAPI and vinculin, and each transwell membrane was mounted on a microscopic slide for visualization and analysis. For colony assays, keratinocytes were dissociated in a single cell solution and mixed 1:1 with matrigel (BD Biosciences). Per well, 3,000 cells were seeded and incubated for 30 min at 37 °C. Colonies were fixed and stained 14 d after seeding. Medium was changed every 4 d.

Proliferation Assay. To determine the proliferation of keratinocytes, cells were stained with Ki-67 as described above. Approximately, 300 cells were counted and scored for Ki-67 positivity per cell type.

Optical Stretcher Measurements. Before measurement, cells cultured at 32 °C and 5% CO_2 were detached using 0.025% Trypsin/EDTA (PAA) and resuspended in culture medium. The cell suspension was then mounted into a fully automated μOS setup where each cell deformation experiment is recorded using video microscopy, based on the setup described by Lincoln et al. (45). Each single suspended cell is delivered via a microfluidic system to the measurement region and trapped between two divergent laser beams followed by a creep experiment: After 1 s of trapping, the laser power is increased in a step-like manner for 2 s (stretch), followed by 2 s of additional trapping (relaxation) (Fig. 1*A*). At the end of each single cell experiment, a new cell is automatically transported to the measurement region. The applied laser pattern for each single cell was the same throughout the whole study (Fig. 1*A*). Experiments were performed at a constant 23 °C stage temperature, which was adjusted via an environmental controller for the

microscope stage. For each cell type (WT, KO, and K5), the corresponding measurement with LatA-treated cells was carried out with the same batch of cells on the same day. Before LatA treatment, different concentrations were tested, where the most effective concentration (0.25 μM) was taken where cells were still viable and relaxed back to normal after removal of LatA (46).

Deformation Data Analysis. The relative deformation data are derived via an automated subpixel edge detection algorithm implemented in Matlab (MathWorks). The algorithm corrects for small angle rotations of the cell in the trap using feature tracking.

All remaining cells are evaluated with respect to their creep deformation $J(t) = \varepsilon(t)/\sigma_0$, where $\varepsilon(t) = [d(t) - d(0)]/d(0)$ is the relative deformation of a cell along the laser axis, and σ_0 is the optically induced stress, which linearly depends on the applied laser power P_{stretch} (Fig. 1*A*) (9, 47).

As a consequence of the non-Gaussian distribution of our optical deformation values for a cell population, the appropriate value for presentation is the median. With the form of the distributions for cell mechanical properties still under debate in the community, bootstrapping is used to estimate the 95%, 99%, and 99.9% CIs for all of the median deformation values presented in this work. Additionally, various distributions were tested but found to give poor results in fitting the distributions of the LatA-treated cells (including lognormal distribution; Fig. S3).

ACKNOWLEDGMENTS. We thank Roland Stange and Tobias Kießling for the implementation of automatic optical stretcher and data evaluation software and Steffen Grosser for fruitful discussions. Work in the T.M.M. laboratory is supported by the Deutsche Forschungsgemeinschaft (MA1316-9/3, MA1316-15, INST 268/230-1), the German Federal Ministry of Education and Research (network EB), and the Translational Center for Regenerative Medicine, Translational Center for Regenerative Medicine, Leipzig (PTJ 0315883). Work in the J.A.K. laboratory was supported by ESF: European Social Foundation, and the graduate school BuildMoNa: building with molecules and nano objects.

1. Fuchs E, Cleveland DW (1998) A structural scaffolding of intermediate filaments in health and disease. *Science* 279(5350):514–519.
2. Herrmann H, Hesse M, Reichenzeller M, Aebi U, Magin TM (2003) Functional complexity of intermediate filament cytoskeletons: From structure to assembly to gene ablation. *Int Rev Cytol* 223:83–175.
3. Fuchs E, Green H (1980) Changes in keratin gene expression during terminal differentiation of the keratinocyte. *Cell* 19(4):1033–1042.
4. Omary MB (2009) "IF-pathies": A broad spectrum of intermediate filament-associated diseases. *J Clin Invest* 119(7):1756–1762.
5. Kumar S, Weaver VM (2009) Mechanics, malignancy, and metastasis: The force journey of a tumor cell. *Cancer Metastasis Rev* 28(1-2):113–127.
6. Wolf K, et al. (2007) Multi-step pericellular proteolysis controls the transition from individual to collective cancer cell invasion. *Nat Cell Biol* 9(8):893–904.
7. Fritsch A, et al. (2010) Are biomechanical changes necessary for tumour progression? *Nat Phys* 6(10):730–732.
8. Rotsch C, Radmacher M (2000) Drug-induced changes of cytoskeletal structure and mechanics in fibroblasts: An atomic force microscopy study. *Biophys J* 78(1):520–535.
9. Guck J, et al. (2005) Optical deformability as an inherent cell marker for testing malignant transformation and metastatic competence. *Biophys J* 88(5):3689–3698.
10. Nawaz S, et al. (2012) Cell visco-elasticity measured with AFM and optical trapping at sub-micrometer deformations. *PLoS ONE* 7(9):e45297.
11. Bausch AR, Kroy K (2006) A bottom-up approach to cell mechanics. *Nat Phys* 2(4): 231–238.
12. Lulevich V, Yang HY, Isseroff RR, Liu GY (2010) Single cell mechanics of keratinocyte cells. *Ultramicroscopy* 110(12):1435–1442.
13. Janmey PA, Euteneuer U, Traub P, Schliwa M (1991) Viscoelastic properties of vimentin compared with other filamentous biopolymer networks. *J Cell Biol* 113(1): 155–160.
14. Wang N, Stamenović D (2000) Contribution of intermediate filaments to cell stiffness, stiffening, and growth. *Am J Physiol Cell Physiol* 279(1):C188–C194.
15. Seltmann K, et al. (2013) Keratins mediate localization of hemidesmosomes and repress cell motility. *J Invest Dermatol* 133(1):181–190.
16. Guck J, et al. (2001) The optical stretcher: A novel laser tool to micromanipulate cells. *Biophys J* 81(2):767–784.
17. Vijayaraj P, et al. (2009) Keratins regulate protein biosynthesis through localization of GLUT1 and -3 upstream of AMP kinase and Raptor. *J Cell Biol* 187(2):175–184.
18. Goldman RD, et al. (1986) Intermediate filament networks: Organization and possible functions of a diverse group of cytoskeletal elements. *J Cell Sci Suppl* 5:69–97.
19. Lazarides E (1980) Intermediate filaments as mechanical integrators of cellular space. *Nature* 283(5744):249–256.
20. Reichelt J, Büssow H, Grund C, Magin TM (2001) Formation of a normal epidermis supported by increased stability of keratins 5 and 14 in keratin 10 null mice. *Mol Biol Cell* 12(6):1557–1568.
21. Coulombe PA, Omary MB (2002) 'Hard' and 'soft' principles defining the structure, function and regulation of keratin intermediate filaments. *Curr Opin Cell Biol* 14(1): 110–122.
22. Wagner OI, et al. (2007) Softness, strength and self-repair in intermediate filament networks. *Exp Cell Res* 313(10):2228–2235.
23. Kreplak L, Bär H, Leterrier JF, Herrmann H, Aebi U (2005) Exploring the mechanical behavior of single intermediate filaments. *J Mol Biol* 354(3):569–577.
24. Plodinec M, et al. (2011) The nanomechanical properties of rat fibroblasts are modulated by interfering with the vimentin intermediate filament system. *J Struct Biol* 174(3):476–484.
25. Maloney JM, et al. (2010) Mesenchymal stem cell mechanics from the attached to the suspended state. *Biophys J* 99(8):2479–2487.
26. Hatzfeld M (2007) Plakophilins: Multifunctional proteins or just regulators of desmosomal adhesion? *Biochim Biophys Acta* 1773(1):69–77.
27. Hofmann I, et al. (2000) Interaction of plakophilins with desmoplakin and intermediate filament proteins: An in vitro analysis. *J Cell Sci* 113(Pt 13):2471–2483.
28. Leung CL, Green KJ, Liem RKH (2002) Plakins: A family of versatile cytolinker proteins. *Trends Cell Biol* 12(1):37–45.
29. Andrä K, Nikolic B, Stöcher M, Drenckhahn D, Wiche G (1998) Not just scaffolding: Plectin regulates actin dynamics in cultured cells. *Genes Dev* 12(21):3442–3451.
30. Karashima T, et al. (2012) Interaction of plectin and intermediate filaments. *J Dermatol Sci* 66(1):44–50.
31. Steinböck FA, Wiche G (1999) Plectin: A cytolinker by design. *Biol Chem* 380(2): 151–158.
32. Magin TM, Vijayaraj P, Leube RE (2007) Structural and regulatory functions of keratins. *Exp Cell Res* 313(10):2021–2032.
33. Coulombe PA, et al. (1991) Point mutations in human keratin 14 genes of epidermolysis bullosa simplex patients: Genetic and functional analyses. *Cell* 66(6): 1301–1311.
34. Coulombe PA, Fuchs E (1993) Epidermolysis bullosa simplex. *Semin Dermatol* 12(3): 173–190.
35. Bonifas JM, Rothman AL, Epstein EH, Jr. (1991) Epidermolysis bullosa simplex: evidence in two families for keratin gene abnormalities. *Science* 254(5035):1202–1205.
36. Brabletz T (2012) To differentiate or not—routes towards metastasis. *Nat Rev Cancer* 12(6):425–436.
37. Knösel T, et al. (2006) Cytokeratin profiles identify diagnostic signatures in colorectal cancer using multiplex analysis of tissue microarrays. *Cell Oncol* 28(4):167–175.
38. Karantza V (2011) Keratins in health and cancer: More than mere epithelial cell markers. *Oncogene* 30(2):127–138.
39. Paladini RD, Takahashi K, Bravo NS, Coulombe PA (1996) Onset of re-epithelialization after skin injury correlates with a reorganization of keratin filaments in wound edge keratinocytes: Defining a potential role for keratin 16. *J Cell Biol* 132(3):381–397.
40. Patel GK, Wilson CH, Harding KG, Finlay AY, Bowden PE (2006) Numerous keratinocyte subtypes involved in wound re-epithelialization. *J Invest Dermatol* 126(2): 497–502.
41. Mazzalupo S, Wong P, Martin P, Coulombe PA (2003) Role for keratins 6 and 17 during wound closure in embryonic mouse skin. *Dev Dyn* 226(2):356–365.
42. Beil M, et al. (2003) Sphingosylphosphorylcholine regulates keratin network architecture and visco-elastic properties of human cancer cells. *Nat Cell Biol* 5(9):803–811.
43. Rotty JD, Coulombe PA (2012) A wound-induced keratin inhibits Src activity during keratinocyte migration and tissue repair. *J Cell Biol* 197(3):381–389.
44. Betz RC, et al. (2006) Loss-of-function mutations in the keratin 5 gene lead to Dowling-Degos disease. *Am J Hum Genet* 78(3):510–519.
45. Lincoln B, et al. (2007) Reconfigurable microfluidic integration of a dual-beam laser trap with biomedical applications. *Biomed Microdevices* 9(5):703–710.
46. Wakatsuki T, Schwab B, Thompson NC, Elson EL (2001) Effects of cytochalasin D and latrunculin B on mechanical properties of cells. *J Cell Sci* 114(Pt 5):1025–1036.
47. Guck J, Ananthakrishnan R, Moon TJ, Cunningham CC, Käs J (2000) Optical deformability of soft biological dielectrics. *Phys Rev Lett* 84(23):5451–5454.